A generalized leaky FxLMS algorithm for tuning the waterbed effect of feedback active noise control systems

Lifu Wu [a,*], Xiaojun Qiu[b], Yecai Guo [a]

[a] School of Electronic & Information Engineering, CICAEET, Nanjing University of Information Science and Technology, Nanjing, 210044, China

[b] Centre for Audio, Acoustics and Vibration, Faculty of Engineering and IT, University of Technology Sydney, Sydney, Australia

Abstract— To tune the noise amplification in the feedback system caused by the waterbed effect effectively, an adaptive algorithm is proposed in this paper by replacing the scalar leaky factor of the leaky FxLMS algorithm with a real symmetric Toeplitz matrix. The elements in the matrix are calculated explicitly according to the noise amplification constraints, which are defined based on a simple but efficient method. Simulations in an ANC headphone application demonstrate that the proposed algorithm can adjust the frequency band of noise amplification more effectively than the FxLMS algorithm and the leaky FxLMS algorithm.

Keywords: Active noise control, leaky, waterbed effect

1. Introduction

Active noise control (ANC) system attenuates unwanted noise by employing the secondary sources, whose outputs are used to interfere destructively with the original primary noise [1, 2]. Over the past decades ANC has attracted considerable interests and several applications have been successful, such as the ANC headphones [3, 4], the ANC headrest [5] and ANC in a yacht environment [6]. Feedforward and feedback structures are two basic structures in ANC systems. In a feedforward structure, the unwanted primary noise is picked up by a reference sensor before it propagates to the secondary sources. In a feedback structure, the ANC controller attempts to attenuate the noise without the reference signal in the feedforward structure.

Corresponding author. Email: wulifu@nuist.edu.cn,

A feedforward structure needs a coherent reference signal. If such a reference signal is not available, a feedback structure is an alternative option [1, 2]. The feedback structure has its own weakness. The first is that its noise attenuation bandwidth is typically narrow, the second is that much efforts are required to guarantee the stability of the feedback structure, and the third is the waterbed effects which claim that it is theoretically impossible to have noise reduction simultaneously at all frequencies. If the noise at some frequencies is suppressed in a feedback ANC system, the noise will be increased at some other frequencies [2].

Many efforts have been made to design feedback ANC systems to have both good noise reduction performance and sufficient stability. For example, Bai et al. introduced the H_∞ optimization technique to synthesize the robust controller [4]. Rafaely et al. presented an H_2/H_∞ feedback controller design method for active sound control in a headrest, where an H_2 performance criterion with H_2 and H_∞ constraints were employed and the design procedure was formulated as a convex programming problem using finite impulse response (FIR) Q-parameterization and frequency discretization, and the programming problem is finally solved by sequential quadratic programming [5].

A different approach was proposed to design the feedback controller by flattening the noise amplification due to the waterbed effect in the whole disturbance amplification frequency band, and the amplification peaks are suppressed to relatively small value for the given disturbance attenuation [7]. In their method, the design of the feedback controller relies on the least squares design criteria with a MATLAB function fdesign.arbmagnphase, which sometimes cause sub-optimal performance due to the trading off of parameters setting. Recently, a feedback ANC system using the wavelet packet FxLMS algorithm is proposed by decomposing the broadband noise into several predictable band-limited sections and controlling each section independently [8]. We proposed a simplified adaptive feedback ANC system which adopts the error signal directly as the reference signal in an adaptive feedforward control system and has advantageous of small computational load, easy implementation, and decoupling between the feedforward and feedback structures [9, 10].

The methods in [4, 5, 7] design the feedback controller by formulating the performance specifications from practice into the optimization problem with various design criteria and constraints, and then use some optimization algorithms to search the solutions. The problem with these methods is that it cannot guarantee to find a global optimal solution and abundant experience and repeated attempts are often required to obtain a satisfactory controller, so they are mainly applied to the offline feedback ANC system design. The methods in [6, 8, 9] are based on the adaptive algorithms and can be applied to the online feedback ANC systems, but the waterbed effect is not considered because it is not easy to merge the waterbed effect related constraints into the adaptive algorithm.

In practical feedback ANC systems, although noise amplification at some frequencies due to the waterbed effect cannot be avoided, it is sometimes desired that the noise amplification in a certain specific frequency range can be minimized while outside that specific frequency range is acceptable or can be further processed. For example, in a feedback ANC headphone, while suppressing the noise at 200~1000 Hz, it is hoped that the noise amplification at the 1500~3000 Hz range can be minimized because the residual noise in this frequency range is annoying. In this design, the noise amplification at the other frequency ranges is acceptable because of the specific characteristics of the primary noise and passive headphone structure.

Therefore there is a need for tuning the frequency band of noise amplification efficiently with adaptive algorithms. Based on the results in our previous papers that the leaky FxLMS algorithm can limit the gain of the adaptive filter and improve the stability of feedback ANC systems [9, 10], this paper extends the leaky FxLMS algorithm to tune the waterbed effect for feedback ANC systems, where the scalar leaky factor of the leaky FxLMS algorithm is replaced by a real symmetric Toeplitz matrix and the elements in the matrix are calculated explicitly according to the waterbed effect constraints.

2. The proposed algorithm

2.1 Derivation of the proposed algorithm

The internal model control (IMC) based feedback ANC system is shown in Fig. 1 (a), which is composed of an error sensor to measure the residual noise $e(n)$, a secondary sound source to generate the canceling signal $y(n)$ for attenuation of the primary noise $d(n)$, a reference signal $x(n)$ is filtered through $\hat{S}(z)$, a model for estimating the secondary path $S(z)$, and a control filter $W(z)$ with L coefficients such as $\mathbf{w}(n) = [w_0(n), w_1(n),\ldots w_{L-1}(n)]^T$. Here the reference signal $x(n)$ is synthesized on the basis of $e(n)$ and the secondary signal $y(n)$ filtered by $\hat{S}(z)$. Fig. 1 (b) shows the simplified adaptive feedback system introduced in [9], where the reference signal comes from the error signal directly. The simplified adaptive feedback system has advantageous in computational load and ease of implementation due to the elimination of the convolution operation required in the IMC based system. The algorithm proposed in this paper can be applied to either the IMC based or the simplified feedback system, thus the two systems are not explicitly discriminated in the following derivation.

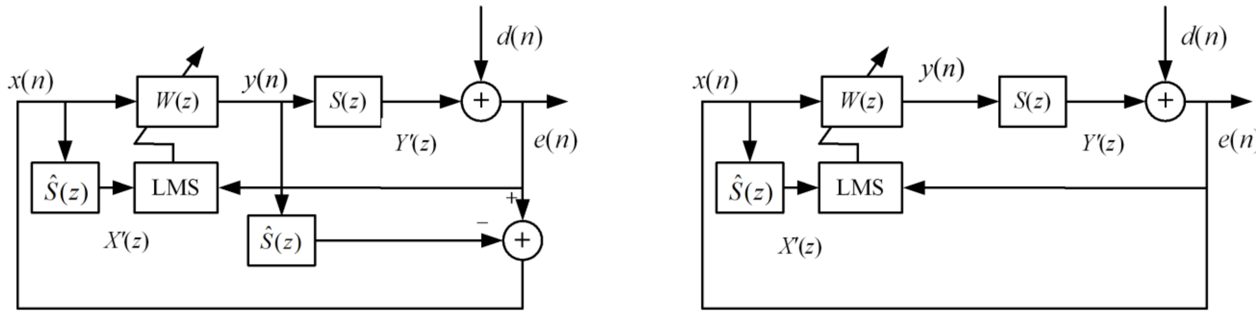

(a) (b)

Fig. 1. Block diagram of adaptive feedback ANC systems, (a) the internal model control based system and (b) the simplified adaptive feedback system in [9].

The cost function of the leaky FxLMS algorithm is [11]

$$J(\mathbf{w}) = e^2(n) + \gamma\, \mathbf{w}^T(n)\mathbf{w}(n) \tag{1}$$

where γ <<1 is a positive number, and

$$\|\mathbf{w}(n)\|^2 = \mathbf{w}^T(n)\, \mathbf{w}(n) \tag{2}$$

Using the gradient descent method, the update equation for $\mathbf{w}(n)$ becomes

$$\mathbf{w}(n+1) = (1-\mu\gamma)\mathbf{w}(n) - \mu e(n)\, \mathbf{x'}(n) \tag{3}$$

where μ is the step-size and $\mathbf{x'}(n)$ is the filtered reference signal which is the linear convolution of the reference signal and impulse response of secondary path. The tap weight vector $\mathbf{w}(n)$ in Eq. (3) finally converges in mean to a biased solution [11], i.e.,

$$\lim_{n\to\infty} E\{\mathbf{w}(n)\} = (\mathbf{R}_{x'x'} + \gamma\mathbf{I})^{-1}\, \mathbf{r}_{dx'} \tag{4}$$

where $\mathbf{R}_{x'x'}$ is the autocorrelation matrix of $\mathbf{x'}(n)$, $\mathbf{r}_{dx'}$ is the cross-correlation between $d(n)$ and $\mathbf{x'}(n)$, and $\mathbf{I}$ is the identity matrix.

The leaky FxLMS algorithm can limit the gain of the adaptive filter $\mathbf{w}(n)$ due to its penalty term $\gamma\|\mathbf{w}(n)\|^2$ in Eq. (1), which ensures that $\mathbf{w}(n)$ achieves a minimum value for $e^2(n)$ and at the same time prevents the term $\|\mathbf{w}(n)\|^2$ from becoming too large. In Eq. (3), $0<1-\mu\gamma<1$, $\mathbf{w}(n)$ is multiplied by $(1-\mu\gamma)$ at each iteration, so $\mathbf{w}(n)$ is not only updated by the gradient related term $e(n)\ \mathbf{x}'(n)$, but also decays to a certain extent at each iteration, which prevents the term $\|\mathbf{w}(n)\|^2$ from becoming too large.

As shown in Fig. 1, the control signal at error sensor in the Z transform domain under the assumption of slow adaptation can be expressed as [9]

$$Y'(\mathrm{z}) = X(\mathrm{z})W(\mathrm{z})S(\mathrm{z}) \approx X'(\mathrm{z})W(\mathrm{z}) \tag{5}$$

The waterbed effect state that the noise amplification is unavoidable in some frequency range for a feedback ANC system, but it can be found from Eq. (5) that if the magnitude frequency response of $W(\mathrm{z})$ in the predefined frequency band is deliberately limited, then the frequency components of $Y'(\mathrm{z})$ in the predefined frequency band can be small and the noise amplification in this frequency band will be alleviated.

Enlightened by the cost function of the leaky FxLMS algorithm, the following cost function is defined,

$$J(\mathbf{w}) = e^2(n) + \gamma\ \mathbf{w}^T(n)\ \mathbf{A}\ \mathbf{w}(n) \tag{6}$$

where $\mathbf{A}$ is an $L \times L$ real symmetric Toeplitz matrix. If $\mathbf{A} = \mathbf{I}$, then Eq. (6) becomes Eq. (1). In order to make $\mathbf{w}^T(n)\mathbf{A}\mathbf{w}(n)>0$, $\mathbf{A}$ must be a positive definite matrix. Using the gradient descent method similarly, the update equation for $\mathbf{w}(n)$ in Eq. (6) is

$$\mathbf{w}(n+1) = (\mathbf{I}-\mu\gamma\mathbf{A})\ \mathbf{w}(n) - \mu e(n)\ \mathbf{x}'(n) \tag{7}$$

The tap weight vector $\mathbf{w}(n)$ in Eq. (7) also converges in mean to a biased solution, i.e.,

$$\lim_{n\to\infty} E\{\mathbf{w}(n)\}=(\mathbf{R}_{\mathrm{x'x'}}+\gamma\mathbf{A})^{-1}\ \mathbf{r}_{\mathrm{dx'}} \tag{8}$$

Let $\mathbf{Q} = \mathbf{I}-\mu\gamma\mathbf{A}$, Eq. (7) is expressed as

$$\mathbf{w}(n+1) = \mathbf{Q}\ \mathbf{w}(n) - \mu e(n)\ \mathbf{x}'(n) \tag{9}$$

where $\mathbf{Q}$ is also a real symmetric Toeplitz and positive definite matrix. Comparing Eq. (9) with Eq. (3), it is found that the scalar leaky factor $(1-\mu\gamma)$ of the leaky FxLMS is replaced by a real symmetric Toeplitz matrix $\mathbf{Q}$, so in the rest of the paper, $\mathbf{Q}$ is named as the leakage matrix.

2.2 The leakage matrix

In order to determine the leakage matrix $\mathbf{Q}$, matrix $\mathbf{A}$ is firstly calculated. Because $\mathbf{A}$ needs to be not only a real symmetric Toeplitz matrix but also a positive definite matrix, $\mathbf{A}$ is selected in this paper to be the autocorrelation matrix of a discrete-time wide-sense stationary random process with real-valued samples $a(n)$, i.e.,

$$\mathbf{A}=\begin{bmatrix} r(0) & r(1) & \dots & r(L-1) \\ r(1) & r(0) & r(1)\dots & r(L-2) \\ \dots & \dots & \dots & \dots \\ r(L-1) & r(L-2) & \dots & r(0) \end{bmatrix} \tag{10}$$

where

$$r(m) = E\{a(n)\, a(n-m)\} \tag{11}$$

According to the Wiener-Khinchin theorem, $r(m)$ can be the inverse discrete time Fourier transform of the power spectral density (PSD) $\varphi(\omega)$ of $a(n)$ [12],

$$r(m)=\frac{1}{2\pi}\int_{-\pi}^{\pi}\varphi(\omega)\, e^{j\omega m}d\omega \tag{12}$$

For real value signal, $r(m) = r(-m)$, $\varphi(\omega) = \varphi(-\omega)$ when $\omega \in [-\pi, \pi]$, so Eq. (12) reduces to

$$r(m)=\frac{1}{\pi}\int_{0}^{\pi}\varphi(\omega)\cos m\omega\, d\omega \tag{13}$$

It should be noted that the elements of matrix **A** can be calculated using Eq. (13) if $\varphi(\omega)$ is defined, for example, if $\varphi(\omega)=1$ (the PSD of white noise), then $r(0) = 1$, $r(m) = 0$ ($m \neq 0$), and $\mathbf{A}=\mathbf{I}$. This is the case of the leaky FxLMS algorithm.

In this paper, in order to deliberately limit the magnitude frequency response of $\mathbf{w}(n)$ in the predefined frequency band, the penalty term $\mathbf{w}^T(n)\mathbf{A}\mathbf{w}(n)$ in Eq. (6) must be given larger weight in that frequency band. A simple but efficient method is selecting the $\varphi(\omega)$ shown in Fig. 2, where $\varphi(\omega)$ can be described by

$$\varphi(\omega)=\begin{cases} q_1, & \omega\in[0,\ \omega_1] \\ \dfrac{q_2-q_1}{\omega_2-\omega_1}(\omega-\omega_1)+q_1, & \omega\in[\omega_1,\ \omega_2] \\ q_2, & \omega\in[\omega_2,\ \omega_3] \\ \dfrac{q_2-q_1}{\omega_3-\omega_4}(\omega-\omega_4)+q_1, & \omega\in[\omega_3,\ \omega_4] \\ q_1, & \omega\in[\omega_4,\ \pi] \end{cases} \tag{14}$$

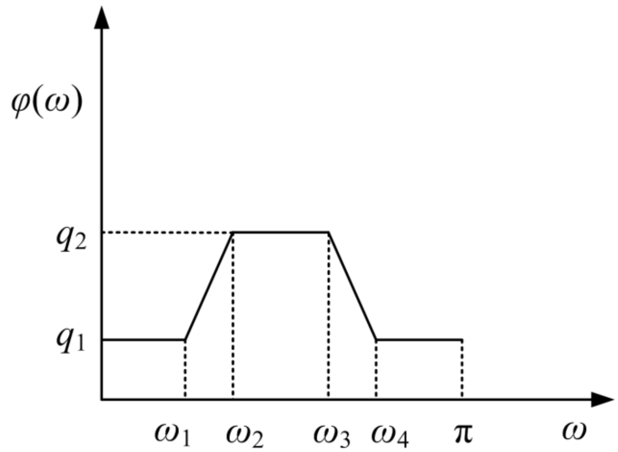

Fig. 2. The piecewise linear power spectral density used to generate the leakage matrix.

Fig. 2 looks like a band-pass filter, ω_2 and ω_3 are the lower and upper cutoff frequencies of a pass-band, respectively and they define the frequency band which the noise amplification should be avoided. ω_1 and ω_4 are the lower and upper frequency of the transition region, respectively. q_1 and q_2 are the magnitude of the pass-band and stop-band respectively.

Substituting Eq. (14) into Eq. (13), the elements of matrix **A** are

$$r(m)=\frac{1}{2\pi}\begin{cases} q_1(\omega_1-\omega_4)+q_2(\omega_3-\omega_2)+0.5(\omega_4+\omega_2-\omega_3-\omega_1)(q_2+q_1)+q_1\pi, & m=0 \\ \dfrac{q_2-q_1}{m^2}\left[\dfrac{1}{\omega_2-\omega_1}(\cos m\omega_2-\cos m\omega_1)+\dfrac{1}{\omega_3-\omega_4}(\cos m\omega_4-\cos m\omega_3)\right], & m\neq 0 \end{cases} \tag{15}$$

In Eqs. (14) (15), ω is the normalized frequency (radius/sample), i.e., $\omega = 0.3\pi$ (radius/sample) corresponds to 2400 Hz if the sampling frequency is 16000 Hz. It can be found that Eq. (14) gives larger weight in the frequency band $[\omega_2, \omega_3]$. Thus if the magnitude frequency response of the controller filter in $[\omega_2, \omega_3]$ band increases a little, the penalty term in Eq. (6) will penalize the cost function $J(\mathbf{w})$ more severely than that at the other frequency bands. This ensures that $\mathbf{w}(n)$ achieves a minimum value for $e^2(n)$ and at the same time prevents the magnitude frequency response of controller filter in $[\omega_2, \omega_3]$ from becoming too large, i.e., the noise amplification in that frequency band is alleviated. After matrix **A** is obtained, the leakage matrix **Q** can be calculated with $\mathbf{Q} = \mathbf{I}-\mu\gamma\mathbf{A}$.

It should be noticed that once $\varphi(\omega)$ is defined, the matrix **A** and **Q** can be calculated in advance of the real time update of $\mathbf{w}(n)$, so the computation of matrix **Q** is not a heavy burden for the proposed algorithm. However, in each iteration, $(1-\mu\gamma)\,\mathbf{w}(n)$ is a product of a scalar and a vector in Eq. (3) for the leaky FxLMS algorithm, while $\mathbf{Q}\mathbf{w}(n)$ is a product of a matrix and a vector for the proposed algorithm. Direct implementing the calculations $\mathbf{Qw}(n)$ requires L^2 multiplications and $L(L-1)$ additions, which may be a heavy burden for the proposed algorithm to be applied in the real time ANC applications. In the proposed algorithm, matrix $\mathbf{A}$ is an $L\times L$ real symmetric Toeplitz matrix, so matrix $\mathbf{Q} = \mathbf{I}-\mu\gamma\mathbf{A}$ is also an $L\times L$ real symmetric Toeplitz matrix.

Fortunately, there are many methods for fast calculation of the products of a Toeplitz matrix and a vector. Some existing fast algorithms are based on embedding the Toeplitz matrix into a circulant matrix of larger size, and calculating the product of the resultant matrix by a vector, then the Toeplitz matrix-vector multiplication can be computed as circulant matrix-vector product [13]. For instance, this product $\mathbf{Qw}(n)$ can be computed using the fast Fourier transform or fast convolution algorithms, and the details of the fast computation can be found in Chapter 16 of [13]. With these fast algorithms, the computation complexity of $\mathbf{Qw}(n)$ can be reduced from $O(L^2)$ to $O(L\log L)$ [13].

3. Simulations and discussions

Simulations were carried out to examine the performance of the proposed algorithm in an ANC headphone application, where the experimental setup was similar to the one described in [3]. As shown in Fig. 3, an active headphone bought from the market was used as the prototype and mounted on a B&K Type 4128C HATS [14], but the original ANC function accompanied with the headphone was disabled. The wires of the reference microphone and error microphone in the headphone were lengthened and passed through the microphone preamplifier, then connected to a B&K Pulse Analyzer. The secondary source (loudspeaker) in the headphone was also connected to the B&K Pulse Analyzer to generate the secondary signal. The B&K Pulse Analyzer was the central device which captured the signals from the reference microphone, error microphone and secondary source, and provided the noise signal to the primary noise source (loudspeaker). A laptop was used to monitor the working states of the other devices and save the data. The sampling frequency of the ANC system is 16000 Hz.

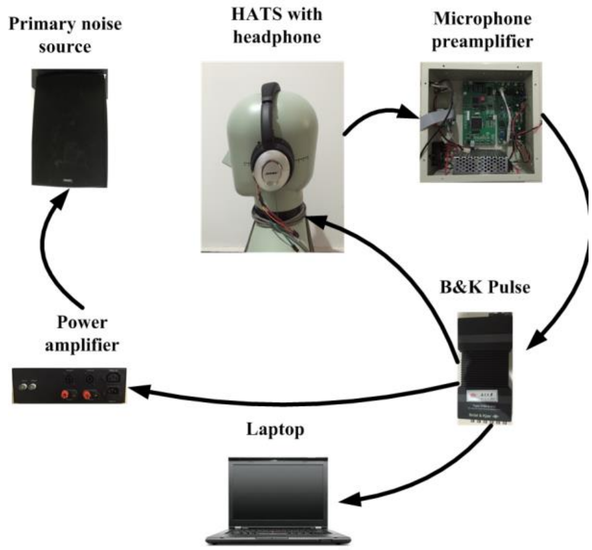

Fig. 3. The connection of the devices in the experiments.

As shown in Fig. 4 (a), the experiments were carried out in an anechoic chamber. A loudspeaker which played back the primary noise is placed in the horizontal plane of the headphone and approximately 40 cm away from the HATS. The measurements were performed for 4 different incident directions of the primary noise (marked with "front", "left", "right" and "rear" in Fig. 4 (b)). The white noise generated by the B&K Pulse was sent to the secondary source and simultaneously this signal and the error microphone signal were recorded, then the secondary path (the impulse response from the input of the secondary source to the output of the error microphone) was estimated using the least mean square (LMS) algorithm. A 256 taps FIR filter was used to estimate the secondary path.

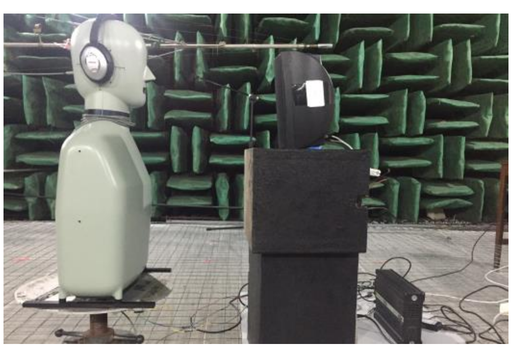

(a)

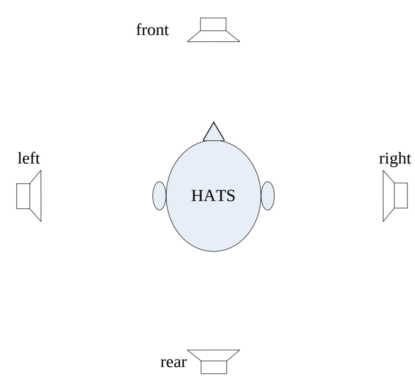

(b)

Fig.4. Diagrammatic view of (a) the experimental configuration in the anechoic chamber, and (b) the 4 different incident directions of the primary noise.

Using the estimated secondary path and the recorded signals of the reference microphone and the error microphone, the "optimal" ANC controllers of the "IMC" feedback system (Fig. 1 (a)) and the "simplified" feedback system (Fig. 1 (b)) were designed respectively, then the difference between the PSD with and without ANC was used to evaluate the noise reduction performance. Detailed performance was tested for the 4 different incident directions respectively, but only the average results of the 4 different incident directions are presented in the remainder of the paper to avoid bothering readers with too many curves.

There are six parameters to be selected in the proposed algorithm. For example, in the simulations, the step-size μ is selected to be 0.004 to ensure fast convergence and good stability, $\gamma = 0.05$; $\omega_2 = 0.3\pi$ and $\omega_3 = 0.5\pi$ for reducing the low frequency noise (below 1500 Hz) and avoid the noise amplification at 2400~4000 Hz in this ANC headphone application, then for transition band, $\omega_1=\omega_2-0.1\pi$ and $\omega_4=\omega_3+0.1\pi$. q_1 and q_2 are two parameters to determine the relative degree of penalty within and outside the frequency band [ω_2, ω_3]. In order to show the influence of q_1 and q_2 on the proposed algorithm, q_1 is fixed with 0.002, q_2 is selected to be 0.02, 0.06 and 0.2 respectively, the noise reduction is shown in Fig. 5. It is found that when the ratio of q_2 and q_1 increases from 10 to 1000, the performance of the proposed algorithm does not vary apparently, and so in the rest of the paper, q_1=0.002, q_2=0.06.

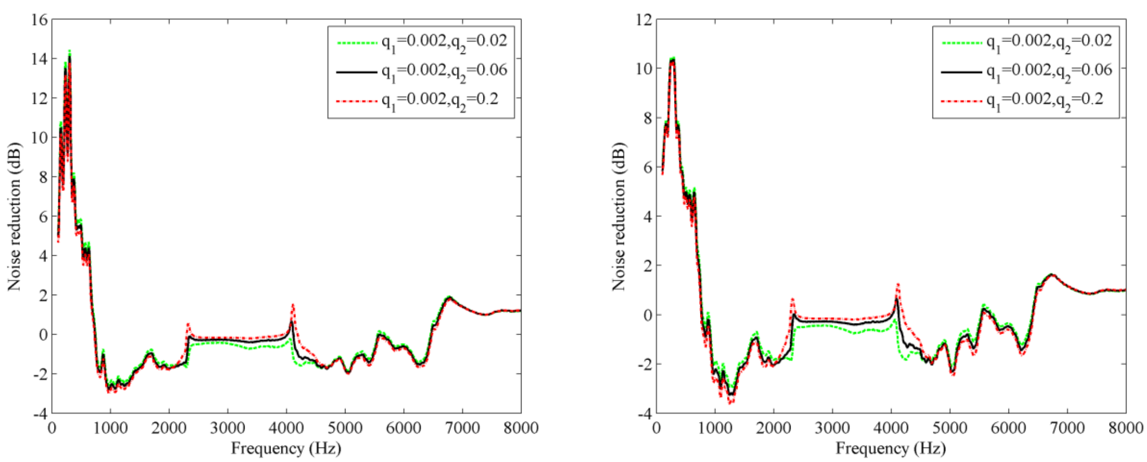

(a) (b)

Fig.5. The noise reduction variation of the proposed algorithm with different parameters setting, (a) internal model control feedback system, and (b) the simplified feedback system.

The FxLMS algorithm, the leaky FxLMS algorithm and the proposed algorithm were utilized to design the ANC controllers of the "IMC" and the "simplified" system respectively. The parameters setting of the 3 algorithms are listed in Table 1. For the FxLMS algorithm, the step-size μ is selected to ensure fast convergence and good stability; for the leaky FxLMS algorithm, $\mu = 0.004$ and $\gamma = 0.05$ which implies the scalar leaky factor in Eq. (3) is 0.9998. Based on the parameters in Table 1 and Eq. (15), the elements $r(m)$ of matrix **A** are calculated and then matrix **Q** is obtained. On the other hand, $\varphi(\omega)$ can also be calculated from the discrete time Fourier transform of $r(m)$ to verify the correctness of the parameters setting of the proposed algorithm. Fig. 6 shows the PSD $\varphi(\omega)$ corresponding to the parameters in Table 1.

Table 1 parameters setting in the FxLMS algorithm, the leaky FxLMS algorithm and the proposed algorithm.

Algorithms	FxLMS	leaky FxLMS	The proposed
Parameters	$\mu = 0.003$	$\mu = 0.004$ $\gamma = 0.05$	$\mu = 0.004$ $\omega_1 = 0.29\pi$, $\omega_2 = 0.3\pi$ $\omega_3 = 0.5\pi$, $\omega_4 = 0.51\pi$ q_1=0.002, q_2=0.06

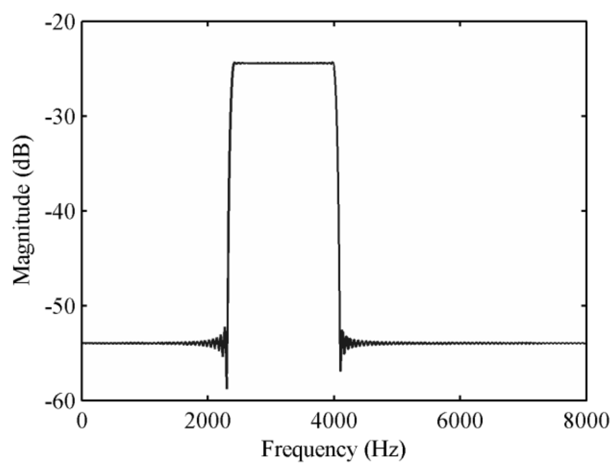

Fig.6. the power spectral density $\varphi(\omega)$ reversely calculated from the elements of matrix **A**.

The performance comparison of the FxLMS algorithm, the leaky FxLMS algorithm and the proposed algorithm are shown in Fig. 7. The results of the IMC feedback system are given in Fig. 7 (a). For the FxLMS algorithm, it is noticed that the attenuation bandwidth is mainly below 2000 Hz, for the 100~700 Hz frequency band, the active noise reduction is larger than 10 dB, the maximum noise reduction is 23 dB located at 300 Hz. For the leaky FxLMS algorithm, the attenuation bandwidth is below 1000 Hz and the maximum active noise reduction is 8 dB located at 300 Hz; For the proposed algorithm, the attenuation bandwidth is also below 1000 Hz and the maximum active noise reduction is 13 dB at 300 Hz frequency.

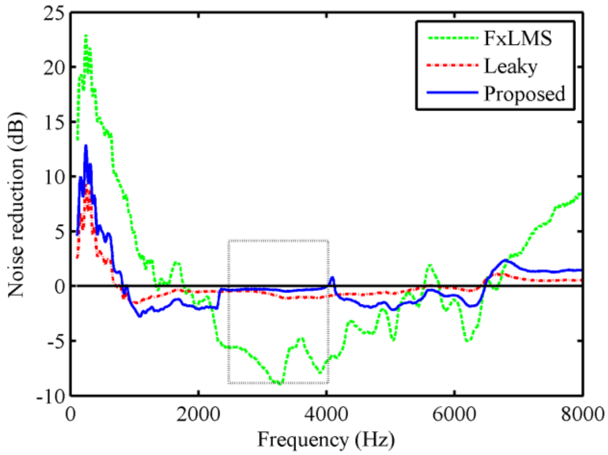

(a)

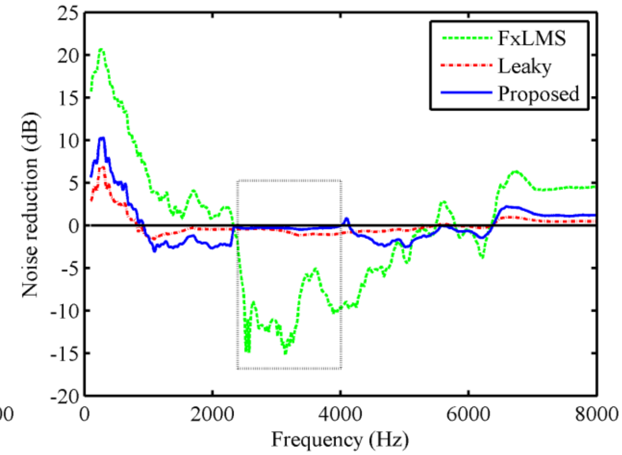

(b)

Fig.7. The ANC performance of the (a) internal model control and (b) the simplified feedback systems based on the FxLMS algorithm, the leaky FxLMS algorithm and the proposed algorithm.

Although the FxLMS algorithm achieves the best noise reduction among the 3 algorithms, its noise amplification is the most serious, especially in the part marked with dotted rectangle in Fig. 7 (a) where in the frequency range of 2400~4000 Hz, there is 5~9 dB noise amplification due to the waterbed effect. The noise amplification of the leaky FxLMS algorithm is less than 2 dB and almost uniformly distributes from 1000 Hz to 7000 Hz frequency band. The noise amplification of the proposed algorithm is less than 4 dB from 1000 Hz to 7000 Hz frequency band, in particular, the noise amplification in the part marked with dotted rectangle is minimized so that it can be neglected.

The results of the simplified feedback system are given in Fig. 7 (b) and it is found that the maximum noise reduction of the FxLMS algorithm, the leaky FxLMS algorithm and the proposed algorithm is 21 dB, 7 dB and 10 dB respectively. Similar to the results in Fig. 7 (a), the noise amplification of the FxLMS algorithm is also the largest among the 3 algorithms. In the part marked with dotted rectangle in Fig. 7 (b), the noise amplification in the frequency range of 2400~4000 Hz is 5~15 dB, which is more serious than the one in Fig. 7 (a). The noise amplification of the leaky FxLMS algorithm is also less than 2 dB and almost uniformly distributes from 1000 Hz to 7000 Hz frequency band. The noise amplification of the proposed algorithm is less than 4 dB from 1000 Hz to 7000 Hz frequency band and in the part marked with dotted rectangle it is the smallest of the 3 algorithms.

From the results in Fig. 7, it is confirmed that the FxLMS algorithm achieves the best noise reduction in the whole frequency range, but its noise amplification is the most serious because the target of the FxLMS algorithm is to minimize $e^2(n)$ without any other constraints. The leaky FxLMS algorithm adds a constraint to the cost function to limit the gain of the controller filter, but the constraint does not differentiate between different frequencies, thus the leaky FxLMS algorithm cannot tune the noise amplification into specific frequencies. The proposed algorithm extends the identity matrix of the leaky FxLMS algorithm to a real symmetric Toeplitz matrix by defining the different penalty weights related to different frequencies, hence it can adjust the noise amplification more effectively in specified frequency range than the leaky FxLMS algorithm. The leaky FxLMS algorithm can regarded as a special case of the proposed algorithm. On the other hand, Eq. (8) indicates that the controller filter of the proposed algorithm converges to a biased solution in comparison with the FxLMS algorithm, so the noise reduction of the proposed algorithm is worse than the FxLMS algorithm.

Fig. 8 shows the magnitude frequency responses of the converged controller filters $\mathbf{w}(n)$ of the 3 algorithms. It is obvious that the magnitude frequency response of $\mathbf{w}(n)$ in the proposed algorithm decays significantly in the 2400~4000 Hz frequency band. This indicates that the magnitude frequency response of $\mathbf{w}(n)$ in the predefined frequency band is deliberately limited, so the noise amplification in that frequency band will be alleviated.

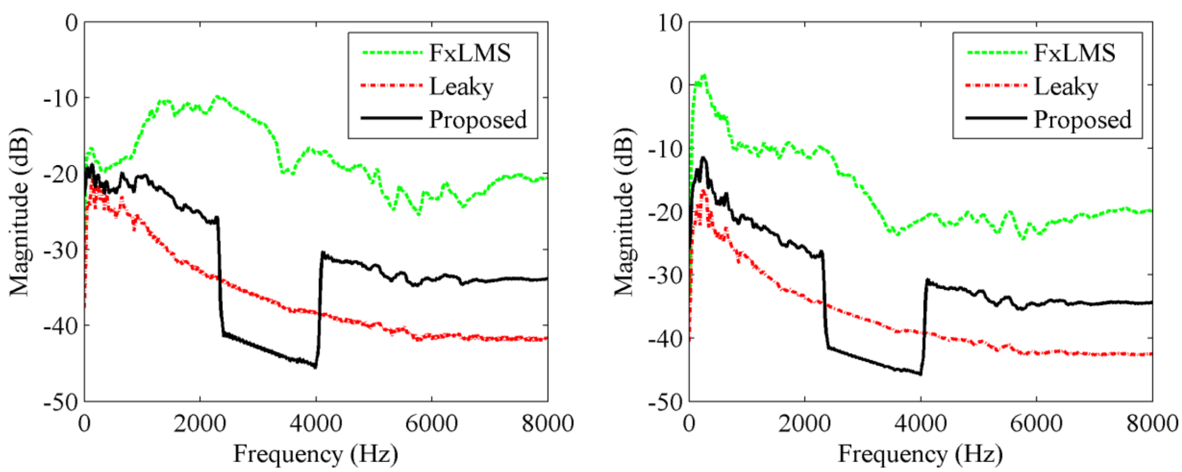

(a) (b)

Fig.8. The magnitude frequency response of the converged controller filters of the FxLMS algorithm, the leaky FxLMS algorithm and the proposed algorithm, in (a) internal model control, and (b) the simplified feedback systems.

4. Conclusions

The waterbed effect state that the noise amplification is unavoidable in the feedback ANC system, in order to effectively tune the noise amplification, a generalized leaky LMS algorithm is proposed in this paper, where the identity matrix of the leaky FxLMS algorithm is replaced by a real symmetric Toeplitz matrix and the elements in the matrix are calculated explicitly by defining the different penalty weights related to different frequencies. Simulation results in a real ANC headphone application demonstrate that if the magnitude frequency response of the controller filter in the target frequency band is deliberately limited, then the noise amplification in that frequency band will be alleviated; The FxLMS algorithm achieves the best noise reduction, but its noise amplification is the most serious, the leaky FxLMS algorithm can limit the noise amplification, but it does not differentiate between different frequencies, thus it cannot tune the noise amplification related to different frequencies, the proposed algorithm can adjust the noise amplification more effectively than the leaky FxLMS algorithm.

Acknowledgment

This project was funded by National Science Foundation of China (11504176) and the Priority Academic Program Development of Jiangsu Higher Education Institutions.

References

[1] S. J. Elliott, *Signal processing for active control*, Academic Press, London (UK), 2001.

[2] C.Hansen, S.Snyder, X. Qiu, L.Brooks, D.Moreau, *Active Control of Noise and Vibration*, Second Edition, CRC Press, 2013.

[3] L. Wu, X. Qiu, J. Ma, Y. Guo, Comparison of feedforward, feedback and hybrid structures on an ANC headphone, *Proceedings of the 23th International Congress on Sound and Vibration*, Athens, Greece, 10–14 July, (2016).

[4] M. Bai, D. Lee, Implementation of an active headset by using the H_∞ robust control theory, *Journal of the Acoustical Society of America* 102 (1997) 2184–2190.

[5] B. Rafaely, S. J. Elliott, H_2/H_∞ active control of sound in a headrest: design and implementation, *IEEE Transactions on Control Systems Technology* 7 (1999) 79–84.

[6] P. Peretti, et al., Adaptive feedback active noise control for yacht environments, *IEEE Transactions on Control Systems Technology* 22 (2014) 737–744.

[7] L. Zhang, L. Wu, X. Qiu, An intuitive approach for feedback active noise controller design, *Applied Acoustics* 74 (2013) 160–168.

[8] L. Luo, J. Sun, B. Huang, A novel feedback active noise control for broadband chaotic noise and random noise, *Applied Acoustics* 116 (2017) 229–237.

[9] L. Wu, X. Qiu, Y. Guo, A simplified adaptive feedback active noise control system, *Applied Acoustics* 81 (2014) 40–46.

[10] L. Wu, X. Qiu, I. Burnett, Y.Guo, Decoupling feedforward and feedback structures in hybrid active noise control systems for uncorrelated narrowband disturbances, *Journal of Sound and Vibration*, 350 (2015) 1–10.

[11] O. J. Tobias, R. Seara, Leaky-FXLMS algorithm: stochastic analysis for Gaussian data and secondary path modeling error, *IEEE Transactions on Speech and Audio Processing*, 13 (2005) 1217–1230.

[12] Petre Stoica, Randolph Moses, *Spectral Analysis of Signals*, Prentice Hall, Upper Saddle River, New Jersey, 2005.

[13] E. Chu, A. George, *Inside the FFT black box: serial and parallel fast Fourier transform algorithms*, CRC Press, 1999.

[14] B&K., Product data-head and torso simulator-type 4128C. Handset positioner for HATS－type 4606: 4 [M], [S.l.]. B&K; (2010).